AIAA JOURNAL
Vol. 31, No. 2, February 1993

Formulation and Solution of Inverse Spaghetti Problem: Application to Beam Deployment Dynamics

Janice D. Downer* and K. C. Park†
University of Colorado, Boulder, Colorado 80309

A finite element model of the dynamics of axially moving, highly flexible beams is presented. The model is based on a geometrically nonlinear beam formulation that allows for large overall motions. To account for the varying length of a deploying beam, a moving finite element reference grid is incorporated within the nonlinear beam formulation such that the number of finite element nodes remains fixed and the finite element length is allowed to vary. Hamilton's law is used to formulate the equations of motion, and a transient integration solution procedure is derived from a space-time finite element discretization of the Hamiltonian variational principle. Computational results of the methodology are presented for a planar inverse-spaghetti problem.

I. Introduction

THE dynamics of axially moving beamlike structures are becoming increasingly important for the analysis of spacecraft and large space structures that deploy flexible appendages such as antenna, stabilizing booms, solar arrays, and long trusslike structures as well as for other applications such as magnetic tape drives, printing machines, traveling cables, and band saws. An extensive amount of research has focused on the modeling of axially moving continua to analyze the dynamic behavior of such structures. One of the most common models of axially moving continua that has received the most attention is the traveling string problem. In what he termed the "spaghetti problem," Carrier[1] analyzed the motion of a string being accelerated upward into a fixed orifice. In other works since then, analytical expressions representing both linear and nonlinear vibrations of axially moving strings subject to various support conditions have been derived.[2-9] The dynamics of beamlike structures traveling between or over fixed supports have also been studied to address industrial applications such as high-speed tape drives and band saws.[10-13] To address spacecraft applications in which antenna or other long flexible structures are deployed from a host satellite, the dynamics of a cantilever beam that is ejected from a single fixed guide are modeled using Bernoulli-Euler beam theory in Ref. 14. In a quite different approach, the extrusion of a beam from a rotating base is modeled using a series of elastically connected rigid links in which the number of rigid links are continuously increased/decreased to account for deployment/retrieval of the beam.[15] General formulations of axially moving Bernoulli-Euler beam models cantilevered to a rotating rigid host body have also been developed to study the effect of appendage deployment on the attitude dynamics of orbiting spacecraft.[16-20] All of these given analyses are based on an assumption of small elastic deformations. With the exception of the discrete spring-mass model of Ref. 15, all of the other models that have been referenced thus far use linear combinations of space-dependent admissible functions of a time-varying length weighted by time-dependent generalized coordinates to represent the displacements of the axially moving beams.

Advanced spacecraft and large space structures are becoming increasingly flexible due to the ever present demand for lightweight structures and the ever increasing size of the structures. To model the behavior of highly flexible structural components, scientists must consider the possibility of large deformations. For this reason, alternative approaches to the deployment problem that move beyond the limiting assumption of small elastic deformations have been presented in recent works. In Ref. 21, the inverse of the spaghetti problem was considered, and a continuum-based formulation of a nonlinear elastica being ejected from a fixed guide at a constant velocity was developed to analyze the motion of a piece of paper being ejected from a copy machine. In Ref. 22, the discrete spring-mass model introduced in Ref. 15 was reformulated in terms of the multibody dynamics order-n algorithms by introducing a variable n for the variable number of links and allowing for unrestricted rotations of the links to approximate large bending-type deformations.

To the best of our knowledge, there exists no general finite element analysis capability for axially moving beams of variable cross sections that are capable of undergoing large overall motions. The objective of this paper is to present a finite element approach to the beam deployment problem to provide such a capability. The present analysis addresses the planar motion of highly flexible beamlike structures being deployed or ejected from a fixed base; a fully three-dimensional analysis of beam ejection from an orbiting base is to be presented in a future work. To allow for large overall motions, the present model is based on the *geometrically exact* beam theories. The geometrically exact beam theories have been presented in recent works to model the dynamics of highly flexible beamlike structures undergoing large overall motions.[23-32] In these theories, the combined rigid-body and deformation motion of a beam is modeled directly with one set of kinematic variables defined with respect to a fixed frame of reference. Nonlinear finite elements that can accommodate large relative displacements between two material points within a beam have been developed from the theory,[24-27,29,30] and the finite element models have been incorporated within computational solution methods developed for multibody dynamic systems.[30-32] By incorporating this type of beam theory to model the deployment problem, significant advances in analysis capabilities can be achieved relative to the formulations based on standard linear representations of beam flexibility as the nonlinear theories allow for large deformations as well as large overall rotations.

In the present work, the deployment motion is accounted for within the nonlinear beam theory by introducing a moving

Presented as Paper 91-1113 at the AIAA/ASME/ASCE/AHS/ASC 32nd Structures, Structural Dynamics, and Materials Conference, Baltimore, MD, April 8-10, 1991; received May 9, 1991; revision received July 8, 1992; accepted for publication July 13, 1992.

*Graduate Research Assistant; currently, Assistant Professor, Department of Engineering Mechanics, University of Wisconsin, Madison, WI 53706. Member AIAA.

†Professor, Department of Aerospace Engineering Sciences. Associate Fellow AIAA.

reference for the kinematic variables. This moving reference is essentially a rigid phantom beam that continually extends with a prescribed deployment speed in a fixed direction. To model the varying beam length, a moving finite element reference grid is employed in which the number of discrete points are fixed and the length of each discrete beam element is allowed to vary. A computational methodology incorporating the variable reference grid is derived from a space-time finite element discretization of a Hamiltonian variational principle. This Hamiltonian-based computational formulation simplifies the numerical treatment of complex convective accelerations that result from the use of a moving reference.

To present the formulation, the rest of the paper is organized as follows. Section II presents the kinematics for the beam deployment problem. The formulation of the equations of motion from Hamilton's law is presented in Sec. III. The space-time finite element discretization of the Hamiltonian formulation is presented in Sec. IV. Section V then presents results of the method for the planar inverse-spaghetti problem.

II. Beam Kinematics

In a geometrically exact beam theory, the complete motion of a beam component undergoing both large rotations and large deformations is described with respect to a frame of reference fixed in space. This type of kinematic modeling is in contrast to the conventional approach widely used in flexible multibody dynamic formulations in which two sets of coordinates, namely, reference and elastic coordinates, are defined to model large overall motions of structural components; reference coordinates model the nominal location and orientation of the component rigid-body motion, and elastic coordinates model small deformations of the components relative to this moving reference using either assumed mode or finite element methods.[33-35] In the geometrically exact approach, the kinematic variables implicitly contain information of both rigid motion and deformations without distinction. Finite strain definitions that are invariant to large rigid-body motions are then developed to define the internal force of an elastically deformed and rotated component as standard linear theories are no longer valid for kinematic variables that contain large rigid-body motions. Along with invariance to rigid-body motions, finite strain definitions model all nonlinear effects such as coupled extensional, flexural, torsional, and transverse shear deformations. In addition, any motion-induced stiffness effects such as the centrifugal stiffness that is experienced during a high-speed rotation of a flexible member are automatically accounted for by the finite strain definitions.

To introduce the geometrically nonlinear theory, a kinematic description for large rotational and deformational motions of a general nondeploying beam that is used in a number of references is described as follows.[23-26,29,30] A space-curved line is introduced to represent the locus of material points defining the beam centroidal axis, and a set of symmetric cross sections are then associated with each material point on this axis. Initially, the beam is straight and untwisted, and the cross sections are perpendicular to the centroidal-axis. A set of reference coordinates $X^T = \{X_1, X_2, X_3\}$ are defined with

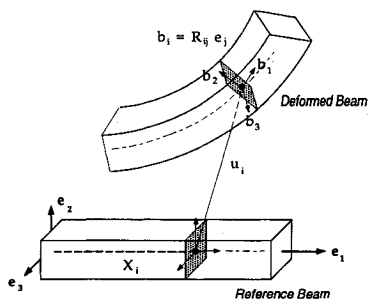

Fig. 1 Spatial beam kinematics.

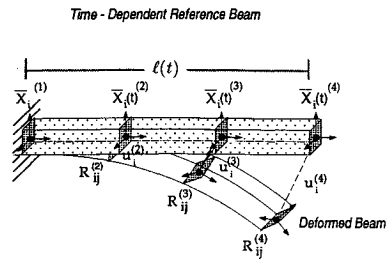

Fig. 2 Time-dependent reference for kinematic variables.

respect to a fixed inertial basis to represent the centroidal axis of this initial configuration. As the beam deforms, this line of centroids assumes a curved line in space, and the cross sections independently assume a new orientation. As shown in Fig. 1, a set of displacement coordinates $u^T = \{u_1, u_2, u_3\}$ is defined to represent the inertial components of the displacement of a material particle on the deformed beam neutral axis with respect to the reference coordinates X. An orthogonal triad of basis vectors $(\boldsymbol{b}_1, \boldsymbol{b}_2, \boldsymbol{b}_3)$ is also assigned to each point on the neutral axis to represent the orientation of the cross-section with respect to the inertial reference frame. The axes $\boldsymbol{b}_2$ and $\boldsymbol{b}_3$ lie in the plane of the cross section, and the axis $\boldsymbol{b}_1$ is normal to the cross section. The origin of the $\boldsymbol{b}$-basis vectors coincides with the centroid of the cross section. The orientation of the cross section does not remain perpendicular to the centroidal axis of the deformed beam due to transverse shear and torsional deformations. An orthogonal transformation matrix R defines the orientation of the $\boldsymbol{b}$-basis vectors with respect to the $\boldsymbol{e}$-basis vectors defined to represent an inertially fixed reference frame such that $\boldsymbol{b}_i = R_{ij}\boldsymbol{e}_j$. The generalized displacements of the beam model referenced to an undeformed fixed configuration are thus a set of translational coordinates u that represent the displacement of the neutral axis and a set of finite rotational coordinates that parameterize the cross section's orientation transformation matrix R.

To model beam deployment in this context, the undeformed beam coordinates X are defined as a function of time $\bar{X}(t)$. The time-dependent inertial coordinates $\bar{X}(t)$, which represent a rigid phantom beam extending from a given point with a prescribed velocity, are defined in a discrete sense as follows. The total length of the rigid phantom beam at any instant in time is defined from the integration over time of a given function $V(t)$ representing the prescribed deployment velocity. A fixed number of moving reference nodes $\bar{X}(t)$ are then defined by spatially dividing the total current length of the rigid phantom beam with an equal number of elements. As shown in Fig. 2, the moving reference nodes are equally positioned between the free end and the boundary along a given fixed direction. The discrete interpretation of the present analysis is thus based on a variable grid finite element approach in which the number of finite element nodes remains fixed and the length of each beam element is allowed to vary. A main advantage of such an approach is that the dimension of a discrete model remains fixed in size; this is in contrast to an alternative approach that would employ a growing number of finite elements of fixed size. In addition, the boundary conditions that are essentially changing with respect to the structure are imposed in a natural manner in the present approach as one nodal point remains fixed at the boundary. The numerical treatment of the variable grid finite element model will be discussed in Sec. IV. The main point of relevance to the present discussion on the kinematics and the derivation of the equations of motion for the beam deployment problem is the fact that the generalized displacements u and R are now defined with respect to and are thus being transported with a set of time-dependent reference coordinates with a prescribed deployment velocity.

To define the velocity of a material particle within the beam configuration, the velocity of transport of variables with the

moving nodes as well as the instantaneous rate of change of the variables must be taken into account. To this end, the total time derivative of the displacement coordinates representing the location of a material point on the deformed neutral axis relative to the moving reference is defined as

$$\frac{Du}{Dt} \equiv \frac{\partial u}{\partial t} + V_i(t)\frac{\partial u}{\partial \bar{X}_i} \tag{1}$$

where $\partial u/\partial t$ represents the particle velocity as measured by an observer moving axially with the beam, $V_i(t) = d\bar{X}_i(t)/dt$ represents the prescribed transport velocity of the reference coordinates, and Du/Dt is the total particle velocity as measured by a fixed observer. In the same manner, the total angular velocity of a particular cross section associated with the neutral axis material point is defined as

$$\omega^D = \omega + V_i(t)k_i \tag{2}$$

where ω is the instantaneous angular velocity of the cross section as seen by an observer traveling with the beam, and k_i is the curvature of the basis vectors attached to the cross section. The angular velocity and curvature vectors are defined in the $\boldsymbol{b}$-basis from the following skew-symmetric tensors:

$$\tilde{\omega} = -\frac{\partial R}{\partial t}R^T, \qquad \tilde{k}_i = -\frac{\partial R}{\partial \bar{X}_i}R^T \tag{3}$$

For planar motion, the nonzero angular velocity component is given as

$$\frac{D\theta}{Dt} \equiv \frac{\partial \theta}{\partial t} + V_i(t)\frac{\partial \theta}{\partial \bar{X}_i} \tag{4}$$

where θ is the planar rotation angle that orients the $\boldsymbol{b}$-frame with respect to an inertial reference frame such that

$$R = \begin{bmatrix} \cos\theta & \sin\theta & 0 \\ -\sin\theta & \cos\theta & 0 \\ 0 & 0 & 1 \end{bmatrix}$$

The position vector locating an arbitrary material point within the deformed planar beam configuration can be described as

$$r = [\bar{X}(t) + u]^T e + \ell_2 b_2 \tag{5}$$

where the notation $e = \{e_1, e_2\}^T$ represents the basis vectors of the inertial reference frame; $\bar{X}^T = \{\bar{X}_1, \bar{X}_2\}$ represents the inertial components of the reference neutral axis position; $u^T = \{u_1, u_2\}$ represents the inertial components of the neutral axis displacement, and ℓ_2 is the distance from the beam neutral axis to an arbitrary material point located on the beam cross section. Likewise, the velocity vector for this material point is given as

$$\frac{Dr}{Dt} = \left(V + \frac{Du}{Dt}\right)^T e - \ell_2 \frac{D\theta}{Dt} b_1 \tag{6}$$

and the variation of the position vector defined in the classic sense of variational calculus as an arbitrary and infinitesimal change in the configuration consistent with the imposed constraints at a fixed instant of time is given as

$$\delta r = \delta u^T e - \ell_2 \delta\theta b_1 \tag{7}$$

To complete the kinematic description, the acceleration vector for the material particle is given as

$$\frac{D^2 r}{Dt^2} = \left(\dot{V} + \frac{D^2 u}{Dt^2}\right)^T e - \ell_2 \frac{D^2\theta}{Dt^2} b_1 - \ell_2 \frac{D\theta^2}{Dt} b_2 \tag{8}$$

where

$$\frac{D^2 u}{Dt^2} = \dot{V}_i + \frac{\partial^2 u}{\partial t^2} + 2V_i\frac{\partial^2 u}{\partial t\,\partial \bar{X}_i} + V_i^2\frac{\partial^2 u}{\partial \bar{X}_i^2} + \dot{V}_i\frac{\partial u}{\partial \bar{X}_i} \tag{9}$$

$$\frac{D^2\theta}{Dt^2} = \frac{\partial^2\theta}{\partial t^2} + 2V_i\frac{\partial^2\theta}{\partial t\,\partial \bar{X}_i} + V_i^2\frac{\partial^2\theta}{\partial \bar{X}_i^2} + \dot{V}_i\frac{\partial \theta}{\partial \bar{X}_i} \tag{10}$$

III. Equations of Motion

From this discussion of the kinematic representation of axially moving beams, we move to a discussion of a suitable formulation of equations of motion for this problem. A fundamental principle of mechanics suited for the application of finite element solution techniques is the principle of virtual work given as

$$\int_\vartheta \left(\rho\delta r \cdot \ddot{r} + \sigma^e : \frac{\partial \delta r}{\partial x} - \delta r \cdot f^e\right) d\vartheta = \int_S \delta r \cdot t\, dS \tag{11}$$

In the previous equation, σ^e is the Cartesian components of the Cauchy stress tensor; x the particle position after some deformation has taken place, ϑ the volume of the deformed beam, ρ the mass density, δr a kinematically admissible virtual displacement, $\ddot{r}$ the acceleration of a material particle, f^e the external force per unit mass, and t the stress vector acting on a surface S.

The principle of virtual work is widely used as a variational source for spatial finite element approximation methods. Application of these techniques to the present analysis will become somewhat complicated due to the previous expression of the virtual work of the inertia forces. As seen in Eqs. (9) and (10), this expression will contain second-order spatial derivatives as well as coupled spatial/temporal derivatives in addition to the second-order time derivatives as a result of the moving reference for the dynamic variables. As such, higher order spatial finite element approximation functions must be employed to form the discrete equations than would have been necessary for a standard fixed reference formulation.

A more natural formulation that readily leads to an attractive computational solution for this type of problem can be derived if Hamilton's law of varying action is used to formulate the equations of motion. Hamilton's law is a weak or variational form in time of the principle of virtual work that transforms the virtual work of the inertia force to first-order form. From this variational statement, a finite element discretization in time can be applied simultaneously with a discretization in space to achieve an attractive numerical treatment of the inertia force of the deploying beam.

To derive Hamilton's law, the principle of virtual work is integrated over an arbitrary time interval $t_1 < t < t_2$ such that the acceleration term can be integrated by parts to lead Eq. (11) to the form

$$\int_{t_1}^{t_2}\int_\vartheta \left(\rho\dot{r}\cdot\delta\dot{r} - \sigma^e : \frac{\partial\delta r}{\partial x} + \delta r \cdot f\right) d\vartheta\, dt = \left(\int_\vartheta \rho\dot{r}\cdot\delta r\, d\vartheta\right)\Bigg|_{t_1}^{t_2} \tag{12}$$

for the present analysis of traction-free surfaces. For the present deployment problem, the inertia term that must be integrated by parts involves the material time derivative definition (6) and a spatial integration over a time dependent volume $\vartheta(t)$ as

$$\int_{t_1}^{t_2}\int_{\vartheta(t)} \rho\frac{D^2 r}{Dt^2}\cdot\delta r\, d\vartheta\, dt, \qquad \frac{D}{Dt} \equiv \frac{\partial}{\partial t} + V_i\frac{\partial}{\partial \bar{X}_i} \tag{13}$$

It can be shown that, by performing a proper interchange of a time derivative and a time-dependent spatial integral as dictated by the Reynold's transport theorum,[36] Hamilton's law

can be extended to address the present moving reference formulation as

$$\int_{t_1}^{t_2}\int_{\vartheta(t)}\left(\rho\frac{\mathrm{D}\boldsymbol{r}}{\mathrm{D}t}\cdot\frac{\mathrm{D}\delta\boldsymbol{r}}{\mathrm{D}t}-\sigma^e:\frac{\partial\delta\boldsymbol{r}}{\partial\boldsymbol{x}}+\boldsymbol{f}\cdot\delta\boldsymbol{r}\right)\mathrm{d}\vartheta\,\mathrm{d}t$$
$$=\int_{\vartheta(t)}\rho\frac{\mathrm{D}\boldsymbol{r}}{\mathrm{D}t}\cdot\delta\boldsymbol{r}\,\mathrm{d}\vartheta\Big|_{t_1}^{t_2} \tag{14}$$

A discussion of the form of the individual terms within this expression in consideration of the beam kinematics variables is given as follows.

The term representing the internal force of a deformed beam

$$\int_{t_1}^{t_2}\int_{\vartheta(t)}\sigma^e:\frac{\partial\delta\boldsymbol{r}}{\partial\boldsymbol{x}}\,\mathrm{d}\vartheta\,\mathrm{d}t\equiv\int_{t_1}^{t_2}\int_{\vartheta(t)}\sigma^e_{ij}\frac{\partial\delta r_i}{\partial x_j}\,\mathrm{d}\vartheta\,\mathrm{d}t \tag{15}$$

is based on the true Cauchy stress representation in which the current deformed beam is used as a reference for all stress and strain measurements. The present formulation is in contrast to a Lagrangian-based approach common within many large rotation/large deformation beam analyses where the stresses and strains are measured with respect to the initial undeformed configuration of the beam.[23-28] Although these Lagrangian formulations are mathematically sound, the Cauchy formulation is based on stress/strain definitions that have physical meaning. In recent work by the present authors, a *convected* coordinate Cauchy-based finite element formulation was developed to model large deformation/large rotation beam dynamics for multibody dynamic applications.[29-31] In the present work, this convected-coordinate formulation will be used to model the internal force within the deploying beam component.

A brief overview of the convected coordinate Cauchy-based formulation for geometrically nonlinear beam analysis is given as follows. The Cauchy stresses and strains are decomposed with respect to convected coordinate directions, shown in Fig. 3, which are defined to lie tangent and perpendicular to the neutral axis of the deformed beam. The convected basis vectors $\boldsymbol{a}=(\boldsymbol{a}_1,\boldsymbol{a}_2,\boldsymbol{a}_3)$ differ from the $\boldsymbol{b}$-basis vectors due to the effects of transverse shear and torsional deformation. The use of a convected frame decomposition of a Cauchy stress representation is motivated by a desire to have a physically meaningful description of the beam deformations that will be conducive to future research involving active control of flexible multibody systems with deployable appendages. The convected reference frame coincides with the coordinate directions of physical strains measured from sensors located and operating on a deformed structure and actual forces to be applied by actuators to induce stress within the deformed structure. As an example, distributed sensors and actuators can be formed by bonding piezoelectric materials to the longitudinal surfaces of a beam component. A voltage applied in the longitudinal direction of a piezoelectric material bonded to the beam surface causes both a longitudinal stress in the direction of the deformed neutral axis of the beam and a bending moment about an axis normal to the deformed beam

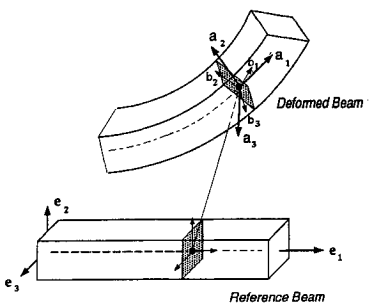

Fig. 3 Convected reference frame.

neutral axis as the net force in the piezoelectric layer acts through the moment arm from the midplane of the layer to the neutral axis of the beam. Such induced and measured stresses physically coincide with the convected frame Cauchy stress model, and this has motivated the use of this particular formulation.

The virtual work of the internal force of a deformed beam can be expressed in terms of convected frame stress tensor components σ^a_{ij}, convected frame spatial coordinates ζ_i, and the convected frame transformation tensor T_{ij} as

$$\int_{\vartheta(t)}\sigma^e_{ij}\frac{\partial\delta r_i}{\partial x_j}\,\mathrm{d}\vartheta=\int_{\vartheta(t)}T_{mi}\frac{\partial\delta r_i}{\partial\zeta_k}\sigma^a_{mk}\,\mathrm{d}\vartheta \tag{16}$$

This can then be written as

$$\int_{\vartheta(t)}T_{mi}\frac{\partial\delta r_i}{\partial\zeta_k}\sigma^a_{mk}\,\mathrm{d}\vartheta=\int_{\xi(t)}(\delta\gamma^TN_\gamma+\delta\kappa^TM_\kappa)\,\mathrm{d}\xi \tag{17}$$

where $\delta\gamma$ is the convected frame components of the membrane and transverse shear strains, $\delta\kappa$ the bending strain, N_γ and M_κ the conjugate resultant stress forces and moments per unit length, respectively, and ξ the convected coordinate tangent to the beam neutral axis. From the derivation in Ref. 29, the virtual strains are given in terms of the beam kinematic variables for the present planar analysis as

$$\delta\gamma=T\frac{\partial\delta u}{\partial\xi}+\begin{Bmatrix}0\\-\delta\theta\end{Bmatrix},\qquad\delta\kappa=\frac{\partial\delta\theta}{\partial\xi} \tag{18}$$

The constitutive laws used within the present formalism to deduce N_γ and M_κ are given as follows. A convected coordinate decomposition of the Truesdell constitutive law, which relates an objective Cauchy stress-rate tensor to an energetically conjugate strain rate tensor, leads to the following resultant stress-strain relations for the planar analysis

$$\dot N_\gamma=\begin{bmatrix}EA&\\&GA\end{bmatrix}\dot\gamma,\qquad\dot M_\kappa=EI\dot\kappa \tag{19}$$

where EA is the axial stiffness, GA the shear stiffness, and EI the bending stiffness. The energetically conjugate strain rate definitions introduced in Eq. (19) are of the same differential operator form as virtual strain definitions given in Eq. (18). The numerical implementation of the previous elastic constitutive law is straightforward as a result of the convected coordinate decomposition; the beam resultant stresses at time t^{n+1} are obtained from the stresses at time t^n via the following additive stress update procedure:

$$N^{n+1}=N^n+\begin{bmatrix}EA&\\&GA\end{bmatrix}\Delta\gamma \tag{20}$$

$$M^{n+1}=M^n+EI\Delta\kappa \tag{21}$$

where $\Delta\gamma$ and $\Delta\kappa$ are incremental strains numerically deduced from the corresponding rate definitions in a manner that is computationally invariant to any large rigid motions contained within the kinematic variables. From this overview, the internal force term within the Hamiltonian equations of motion is given as

$$\int_{t_1}^{t_2}\int_{\vartheta(t)}\sigma^e_{ij}\frac{\partial\delta r_i}{\partial x_j}\,\mathrm{d}\vartheta\,\mathrm{d}t=\int_{t_1}^{t_2}\int_{\xi(t)}\{\delta\gamma^T\ \delta\kappa^T\}\begin{Bmatrix}N_\gamma\\M_\kappa\end{Bmatrix}\mathrm{d}\xi\,\mathrm{d}t \tag{22}$$

Further details of the formulation and computational implementation of this convected coordinate Cauchy formulation for large deformation/large rotation beam dynamics are given in Refs. 29-31.

The terms within Hamilton's law representing the inertia forces of a deploying beam are given as

$$\int_{t_1}^{t_2}\int_{\vartheta(t)} \rho \frac{\mathrm{D}\boldsymbol{r}}{\mathrm{D}t}\cdot\frac{\mathrm{D}\boldsymbol{r}}{\mathrm{D}t}\,\mathrm{d}\vartheta\,\mathrm{d}t = \int_{t_1}^{t_2}\int_{\xi(t)} \frac{\mathrm{D}\bar{u}}{\mathrm{D}t}\cdot M\frac{\mathrm{D}\delta\bar{u}}{\mathrm{D}t}\,\mathrm{d}\xi\,\mathrm{d}t \quad (23)$$

$$\left[\int_{\vartheta(t)} \rho\frac{\mathrm{D}\boldsymbol{r}}{\mathrm{D}t}\cdot\delta\boldsymbol{r}\,\mathrm{d}\vartheta\right]\Bigg|_{t_1}^{t_2} = \left[\int_{\xi(t)}\frac{\mathrm{D}\bar{u}}{\mathrm{D}t}\cdot M\delta\bar{u}\,\mathrm{d}\xi\right]\Bigg|_{t_1}^{t_2} \quad (24)$$

The first expression, Eq. (23), will be referred to as the interior inertia term, and the second expression, Eq. (24), will be referred to as the boundary inertia term. In these expressions, the notation $\bar{u}$ has been employed to represent the two neutral axis displacements and the angular orientation as $\bar{u}^T \equiv \{u_1, u_2, \theta\}$, and M represents the area and inertia properties of the beam cross section as

$$M = \mathrm{diag}\{m,\ m,\ J\}$$

$$m = \int_A \rho\,\mathrm{d}A, \qquad J = \int_A \rho\ell_2^2\,\mathrm{d}A$$

where A is the area of the beam cross-section.

The convective velocity terms can be expressed in terms of convected spatial coordinates ζ_i as opposed to the inertial coordinates $\bar{X}_i$ introduced in Eq. (1) as

$$\frac{\mathrm{D}\bar{u}}{\mathrm{D}t} = \frac{\partial\bar{u}}{\partial t} + v_i^a\frac{\partial\bar{u}}{\partial\zeta_i}, \qquad v_i^a \equiv T_{ij}V_j \quad (25)$$

Now the nodal displacements u locating the deformed neutral axis are solely a function of the a_1 convected coordinate that is tangent to the deformed neutral axis $\xi \equiv \zeta_1$. Likewise, as the plane of the cross section strictly rotates without any warping deformation, the nodal orientations θ are also solely a function of the convected tangent coordinate ξ. As such, the total velocity definition can be simplified to

$$\frac{\mathrm{D}\bar{u}}{\mathrm{D}t} = \frac{\partial\bar{u}}{\partial t} + V^a\frac{\partial\bar{u}}{\partial\xi}, \qquad V^a = T_{1j}V_j \quad (26)$$

when applied to the present kinematic description given in Eq. (5). This latter velocity expression is preferred as it is consistent with the present beam formulation that is based on convected coordinate stress and strain definitions. In this manner, a consistent finite element approximation of the spatial derivatives within both the inertia and internal force terms can be achieved.

The final term within the Hamiltonian equations to be discussed corresponds to the external force acting on the beam component. One application of the present analysis is the inverse spaghetti problem in which a very flexible beam is ejected from a rigid horizontal guide into a uniform gravitational field. For this case, the external force is simply

$$\int_{t_1}^{t_2}\int_{\vartheta(t)} \delta r_i f_i\,\mathrm{d}\vartheta\,\mathrm{d}t = \int_{t_1}^{t_2}\int_{\xi(t)} \rho A u_2 g\,\mathrm{d}\xi\,\mathrm{d}t \quad (27)$$

where g is the acceleration due to gravity at the earth's surface.

IV. Space-Time Discretization of Hamiltonian Equations

From the Hamiltonian equations of motion, an accurate numerical solution procedure is derived from a simultaneous finite element approximation over both the space and time domains. To this end, the generalized displacement $\bar{u}$ is approximated between two points in space ξ_1 and ξ_2 and two points in time t_1 and t_2 by the following bilinear function in space and time as

$$\bar{u} \simeq \left(1-\frac{\xi}{\ell}\right)\left(1-\frac{t}{h}\right)\bar{u}_{\xi_1}^{t_1} + \left(1-\frac{\xi}{\ell}\right)\left(\frac{t}{h}\right)\bar{u}_{\xi_1}^{t_2} + \left(\frac{\xi}{\ell}\right)\left(1-\frac{t}{h}\right)\bar{u}_{\xi_2}^{t_1} + \left(\frac{\xi}{\ell}\right)\left(\frac{t}{h}\right)\bar{u}_{\xi_2}^{t_2} \quad (28)$$

where

$$0 \le \xi \le \ell, \qquad \ell = \xi_2 - \xi_1$$

$$0 \le t \le h, \qquad h = t_2 - t_1$$

and the notation $\bar{u}_{\xi_I}^{t_J}$ corresponds to the value of $\bar{u}$ at a spatial nodal position ξ_I and the point in time t_J. The discrete values $\bar{u}_{\xi_I}^{t_J}$ are defined with respect to the moving coordinate $\bar{X}_I(t_j)$ of the rigid phantom beam that is prescribed throughout the simulation as a function of the deployment speed. The linear C_0 continuous approximating functions employed in Eq. (28) for both the spatial domain ξ and the time domain t are sufficient for the present analysis as the spatial and temporal derivatives within the Hamiltonian variational statement are no higher than first order. With the approximation (28), the Hamiltonian variational equations can be transformed to a finite set of algebraic equations to be solved for the unknown nodal variables $\bar{u}_I^J$. The resulting algebraic equations are nonlinear due to the geometrically nonlinear beam analysis, and a Newton-Raphson iteration algorithm is required for their solution.

The algebraic equations take the following form.The interior inertia term Eq. (23) within the Hamiltonian variational statement is approximated as

$$\int_{t_1}^{t_2}\int_{\xi(t)} \left(\frac{\partial\bar{u}^T}{\partial t} + V^a\frac{\partial\bar{u}}{\partial\xi}\right)^T M\left(\frac{\partial\delta\bar{u}}{\partial t} + V^a\frac{\partial\delta\bar{u}}{\partial\xi}\right)\mathrm{d}\xi\,\mathrm{d}t \simeq \{\delta\bar{u}_d^{t_1^T}\ \delta\bar{u}_d^{t_2^T}\}\begin{bmatrix}A_{11} & A_{12}\\ A_{21} & A_{22}\end{bmatrix}\begin{Bmatrix}\bar{u}_d^{t_1}\\ \bar{u}_d^{t_2}\end{Bmatrix} \quad (29)$$

In this expression, the subscript d on the variables $\bar{u}_d^{t_i}$, $i = 1, 2$, represents the generalized displacements (u_1, u_2, θ) at the given time stations t_i for the entire set of n_ξ spatial finite element nodes used to discretize the deploying beam length. The terms A_{11}, A_{12}, A_{21}, and A_{22} are $(3n_\xi) \times (3n_\xi)$ block matrices given as

$$A_{11} = \frac{1}{h}M_1 + M_2 + M_2^T + \frac{h}{4}M_3 \quad (30a)$$

$$A_{12} = -\frac{1}{h}M_1 + M_2 - M_2^T + \frac{h}{4}M_3 \quad (30b)$$

$$A_{21} = -\frac{1}{h}M_1 - M_2 + M_2^T + \frac{h}{4}M_3 \quad (30c)$$

$$A_{22} = \frac{1}{h}M_1 - M_2 - M_2^T + \frac{h}{4}M_3 \quad (30d)$$

where the matrices M_i, $i = 1, 3$ are derived from standard displacement finite element evaluations of the terms

$$\int_\xi \frac{\partial\delta\bar{u}^T}{\partial t}M\frac{\partial\bar{u}}{\partial t}\,\mathrm{d}\xi \simeq \delta\dot{u}_d^T M_1\dot{u}_d \quad (31a)$$

$$\int_\xi V^{a^2}\frac{\partial\delta\bar{u}^T}{\partial\xi}M\frac{\partial\bar{u}}{\partial\xi}\,\mathrm{d}\xi \simeq \delta\bar{u}_d^T M_3\bar{u}_d \quad (31b)$$

$$\int_\xi V^a\frac{\partial\delta\bar{u}^T}{\partial t}M\frac{\partial\bar{u}}{\partial\xi}\,\mathrm{d}\xi \simeq \delta\dot{u}_d^T M_2\bar{u}_d \quad (31c)$$

obtained from a linear spatial approximation

$$\bar{u} \simeq \left(1 - \frac{\xi}{\ell}\right)\bar{u}_{\xi_1} + \left(\frac{\xi}{\ell}\right)\bar{u}_{\xi_2} \tag{32}$$

for the displacements $\bar{u}$ as well as for the variables $\delta\bar{u}$, V^a, $\dot{u} \equiv d\bar{u}/dt$, and $\delta\dot{u}$.

The boundary inertia term Eq. (24) within the Hamiltonian variational statement is evaluated as follows. The term is first rewritten as

$$\int_{\xi(t)} \frac{D\bar{u}}{Dt} \cdot M\delta\bar{u}\, d\xi \Big|_{t_1}^{t_2} = \int_{\xi(t)} \delta\bar{u}^T P_{\dot{u}}\, d\xi \Big|_{t_1}^{t_2} \tag{33}$$

where

$$P_{\dot{u}} \equiv M\left(\frac{\partial\bar{u}}{\partial t} + V^a\frac{\partial\bar{u}}{\partial\xi}\right) \tag{34}$$

is the vector of generalized momenta. To achieve a correct numerical evaluation of the boundary term, the expression (33) is evaluated exactly in the time domain and is approximated only in the spatial domain. As such, the approximation of the boundary inertia term is given as

$$\int_{\xi(t)} \delta\bar{u}^T P_{\dot{u}}\, d\xi \Big|_{t_1}^{t_2} \simeq \{\delta\bar{u}_d^{t_1^T}\ \ \delta\bar{u}_d^{t_2^T}\}\begin{bmatrix} -C^{t_1} & 0 \\ 0 & C^{t_2}\end{bmatrix}\begin{Bmatrix} P_{\dot{u}_d}^{t_1} \\ P_{\dot{u}_d}^{t_2}\end{Bmatrix} \tag{35}$$

where the matrix C^{t_i} is obtained from a standard finite element evaluation of the spatial integral over the length $\xi(t_i)$ given in Eq. (33) using the linear finite element approximations

$$\delta\bar{u}^{t_i} \simeq \left(1 - \frac{\xi}{\ell}\right)\delta\bar{u}_{\xi_1}^{t_i} + \left(\frac{\xi}{\ell}\right)\delta\bar{u}_{\xi_2}^{t_i}$$

$$P_{\dot{u}_d}^{t_i} \simeq \left(1 - \frac{\xi}{\ell}\right)P_{\dot{u}_d\xi_1}^{t_i} + \left(\frac{\xi}{\ell}\right)P_{\dot{u}_d\xi_2}^{t_i}$$

for the virtual displacements ($\delta\bar{u}^{t_1}$ and $\delta\bar{u}^{t_2}$) and the generalized momenta ($P_{\dot{u}_d}^{t_1}$ and $P_{\dot{u}_d}^{t_2}$). The evaluation of this boundary term with a discrete momentum variable is necessary to achieve an unconditionally stable time-domain integration scheme from a discretization of Hamilton's law.[37,38] The evaluation also provides an exact discrete interpretation of the impulse-momentum principle and thus recovers the momenta at the end of each time step based on physical principles.

The space-time finite element approximation of the internal force is given as

$$\int_{t_1}^{t_2}\int_{\xi(t)} \{\delta\gamma^T\ \ \delta\kappa^T\}\begin{Bmatrix} N_\gamma \\ M_\kappa\end{Bmatrix} d\xi\, dt \simeq \{\delta\bar{u}_d^{t_1^T}\ \ \delta\bar{u}_d^{t_2^T}\}\begin{Bmatrix} \frac{h}{2} & S_u \\ \frac{h}{2} & S_u\end{Bmatrix} \tag{36}$$

In this expression, S_u represents a nonlinear spatial finite element evaluation of the internal force of the beam as

$$\int_{\xi(t)} \{\delta\gamma^T\ \ \delta\kappa^T\}\begin{Bmatrix} N_\gamma \\ M_\kappa\end{Bmatrix} d\xi \simeq \delta\bar{u}_d^T S_u \tag{37}$$

The nodal internal force S_u is a nonlinear function of the nodal displacements and rotations $\bar{u}_d^{t_1}$ and $\bar{u}_d^{t_2}$. The computation of the nodal internal force S_u from the generalized nodal degrees of freedom $\bar{u}_d^{t_i}$ at a given point in time is presented in previous work of Downer,[29] Downer et al.,[30] and Park et al.[31]

In deriving Eq. (36), reduced one-point integration methods were employed to evaluate both the integration over the changing spatial domain and the integration over the time interval. As a result, the factor $h/2$ where $h = t_2 - t_1$ appears in the approximation, and S_u is evaluated at the mid-point in time $t_h = t_1 + h/2$ using nodal displacements and rotations $\bar{u}_d^{t_h}$ that are the average of $\bar{u}_d^{t_1}$ and $\bar{u}_d^{t_2}$. In general, it has been shown that an exact evaluation of the space-time finite element approximation for the basic kinematic or *primal* form of Hamilton's law employed within leads to conditionally stable time integration algorithms such that small step sizes may be required to achieve accurate results.[37,39-41] This type of behavior is similar to the locking phenomenon witnessed during the use of certain elasticity finite elements for static analysis that has been attributed to inconsistencies in the order of approximation of various strain energy terms. As with the locking phenomenon, it was discovered that inaccurate reduced integrations in time of the higher order terms will lead to unconditionally stable time integration algorithms. Space-time finite element discretizations of a *mixed* form of Hamilton's law have also resulted in algorithms with unconditionally stable numerical behavior.[40,41] The former approach has been adopted in the present analysis.

A brief overview of the computation of the nodal internal forces S_u is given as follows. A set of incremental constant element strains are computed from a set of incremental displacements and rotations defined for the planar case as

$$\Delta\bar{u}_d = \bar{u}_d^{t_2} - \bar{u}_d^{t_1} \tag{38}$$

The incremental strains approximate an integration of the strain rate definitions over a single time step in a manner that is invariant to any rigid motions experienced by the system. Given the computed incremental strains, the resultant stresses are obtained via an appropriate stress update procedure given in Eqs. (20) and (21), and the element internal force is then formed from a spatial finite element discretization of the strain-displacement operator. For each finite element, these incremental strains and resultant stresses are computed with respect to a convected reference frame defined within the element. For two-noded constant strain beam elements, the a_1 tangent axis of the convected reference frame lies along the straight line connecting the two element nodes.

It is important to note here that in the present moving node formulation the coordinates $\bar{u}_d^{t_1}$ and $\bar{u}_d^{t_2}$ are defined with respect to different spatial grids; the coordinates $\bar{u}_d^{t_1}$ are defined with respect to the nodes $\bar{X}(t_1)$, whereas the coordinates $\bar{u}_d^{t_2}$ are defined with respect to the nodes $\bar{X}(t_2)$. Before averaging these coordinates for the one-point integration evaluation, the coordinates $\bar{u}_d^{t_1}$ must be extrapolated to the grid $\bar{X}(t_2)$. This extrapolation is also necessary for the stress update procedure as the incremental displacements must also be computed from variables defined on a consistent grid. To this end, the displacements $\bar{u}_d^{t_1}$ are extrapolated to a new value $\bar{u}_d^{t_1\prime}$ defined relative to the grid $\bar{X}(t_2)$ as follows. The first node of the phantom beam remains fixed at a defined origin such that $\bar{X}_1(t_1) = \bar{X}_1(t_2)$, and thus $\bar{u}_1^{t_1\prime} = \bar{u}_1^{t_1}$. From this first node, the rest of the displacements of the finite element model can be sequentially obtained for the remaining spatial nodes $i = 2, \ldots, n_\xi$ contained within $\bar{u}_d^{t_1}$ as

$$\bar{u}_{i+1}^{t_1\prime} = \bar{u}_i^{t_1\prime} + \frac{\ell_X^{t_2}}{\ell_X^{t_1}}(\bar{u}_{i+1}^{t_1} - \bar{u}_i^{t_1}) \tag{39}$$

where $\ell_X^{t_i}$ represents the length between two nodes of the phantom beam at the given instant of time t_i; this length is automatically prescribed for a constant deployment speed V as

$$\ell_X^{t_i} = \bar{X}_{i+1}(t_i) - \bar{X}_i(t_i) = \frac{Vt_i}{n_{\text{ele}}} \tag{40}$$

where n_{ele} is the fixed number of variable length finite elements. This extrapolation scheme was developed such that the element convected reference frames, which lie along the straight line connecting the two nodes of an element in the deformed beam state, defined by the extrapolated nodal position coordinates $\bar{X}(t_2) + u_d^{t_1\prime}$, are identical to the convected reference frames that were computed from the original deformed position coordinates $\bar{X}(t_1) + u_d^{t_1}$. With this particular scheme, the incremental convected frame stress update proce-

dure is oblivious to the extrapolation.This is important when implementing the previously developed internal force computation for the present beam deployment analysis using variable length finite elements.

To complete the discrete approximation, the external body forces acting on the beam are derived in a manner similar to the internal force as

$$\int_{t_1}^{t_2}\int_{\vartheta(t)} \delta r_i f_i \, d\vartheta \, dt \simeq \{\delta\bar{u}_d^{t_1^T} \;\; \delta\bar{u}_d^{t_2^T}\} \begin{Bmatrix} \frac{h}{2} & F_G \\ \frac{h}{2} & F_G \end{Bmatrix} \tag{41}$$

where F_G corresponds to a standard displacement finite element evaluation of

$$\int_{\xi(t)} \rho A \, \delta u_2^T g \, d\xi \simeq \delta\bar{u}_d^T F_G \tag{42}$$

using a linear displacement, Eq. (32). As with the internal force evaluation, a one-point Gaussian integration in time is employed to arrive at Eq. (41).

By combining all of the approximations, namely, that of the interior inertia term, Eq. (29), the boundary inertia term, Eq. (35), the internal force term, Eq. (36), and the external force term, Eq. (41), we arrive at the following set of algebraic equations:

$$A_{11}\bar{u}_d^{t_1} + A_{12}\bar{u}_d^{t_2} - \frac{h}{2}S_u + \frac{h}{2}F_G = -C^{t_1}P_{\dot{u}_d}^{t_1} \tag{43}$$

$$A_{21}\bar{u}_d^{t_1} + A_{22}\bar{u}_d^{t_2} - \frac{h}{2}S_u + \frac{h}{2}F_G = C^{t_2}P_{\dot{u}_d}^{t_2} \tag{44}$$

which represent the space-time discretization of the Hamilton variational statement.

This space-time finite element discretization of the Hamilton variational statement leads to the following step-by-step implicit time integration algorithm. It is readily seen that, given a set of initial conditions for the discrete generalized displacements $\bar{u}_d^{t_1}$ and the generalized momenta $P_{\dot{u}_d}$, the first set of equations, Eq. (43), can be solved for the generalized displacements at the time t_2. Given this solution for $\bar{u}_d^{t_2}$, the second set of equations, Eq. (44), can then be solved for the generalized momenta $P_{\dot{u}_d}$ at time t_2. These new solutions can then be used as initial conditions for the next step in time, and the process can be repeated to give a one-step implicit time integration algorithm.

As the first algebraic equation is nonlinear due to the finite deformation beam model, a Newton-Raphson iterative procedure must be employed to obtain the solution for the generalized displacements $\bar{u}_d^{t_2}$. To this end, a linearized set of equations

$$E_{(k)}\Delta\bar{u}_{d(k+1)}^{t_2} = -r_{(k)} \tag{45}$$

where

$$r_{u_{(k)}} = A_{11}\bar{u}_d^{t_1} + A_{12}\bar{u}_{d(k)}^{t_2} - \frac{h}{2}S_{u_{(k)}} + \frac{h}{2}F_{G_{(k)}} + C^{t_1}P_{\dot{u}_d}^{t_1}$$

is the residual errors of the algebraic equations (43) at the solution $\bar{u}_{d(k)}^{t_2}$ obtained for the kth iteration, and

$$E \equiv A_{12} - \frac{h}{4}K^S \tag{46}$$

is the tangent solution matrix. The term K^S represents the tangent stiffness matrix for the nonlinear internal force term

$$\delta F^S \equiv \int_{\xi(t)} \{\delta\gamma^T \;\; \delta\kappa^T\} \begin{Bmatrix} N_\gamma \\ M_\kappa \end{Bmatrix} d\xi$$

and this tangent stiffness matrix is derived in Ref. 29. Given the solution matrix E for the Newton-Raphson iteration procedure, the linearized equations are solved at each iteration for incremental displacements $\Delta\bar{u}_d^{t_2}$. These incremental solutions are then used to update the displacements $\bar{u}_{d(k)}^{t_2}$ for the next iteration via

$$\bar{u}_{d(k+1)}^{t_2} = \bar{u}_{d(k)}^{t_2} + \Delta\bar{u}_{d(k+1)}^{t_2} \tag{47}$$

and the procedure is repeated until a converged solution for $\bar{u}_d^{t_2}$ is found. Given a solution for $\bar{u}_d^{t_2}$, the generalized momenta $P_{\dot{u}_d}^{t_2}$ can then be found from a direct solution of Eq. (44). These solutions, namely, the generalized displacements $\bar{u}_d^{t_2}$ and the generalized momenta $P_{\dot{u}_d}^{t_2}$, then become the initial conditions for the next step in time.

V. Results

We now give some numerical results of the proposed formulation and computational solution procedure. To illustrate the capabilities of the present procedure, a simulation of a beam being ejected from a rigid horizontal guide into a uniform gravitational field as shown in Fig. 4 is presented as follows. In this example, the beam material parameters of $\rho A = 5.9 \times 10^{-5}$ lbm/in., $EA = 939$ lb, $GA = 450$ lb, $EI = 0.7825$ lb in.^{2}, and total length $\ell = 11$ in. when fully deployed are chosen. These parameters are chosen to model a beam with flexibility on the order of that of a sheet of paper. Such an analysis simulating the ejection of a piece of paper from a fixed guide was performed in Ref. 21 in which the end orbits of a nonlinear elastica model issuing from a rigid horizontal guide at a constant velocity into a uniform gravitational field are presented. In this particular reference, a dimensionless weight-to-stiffness ratio $\mu = mg\ell^4/EI$ and a dimensionless velocity $v = V\ell\sqrt{m\ell/EI}$ where m is a mass per unit surface area, g is the acceleration of gravity, ℓ is the total length, and EI, the bending stiffness, and V, the constant ejection velocity, are used to parameterize the elastica model and the end-orbit solution. The beam parameters just given were chosen to coincide with the value of $\mu = 50$ used in Ref. 21 to model the flexibility of a sheet of paper. The so-called beam end-orbit, or the x-y coordinates of the beam tip throughout the deployment, as obtained by the present algorithm are shown for the dimensionless ejection velocities of $v^2 = 100$, 50, and 20; these parameters correspond to an actual velocity of $V = 92$, 65, and 41 in./s, respectively. The results obtained from the pre-

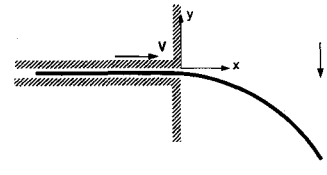

Fig. 4 Beam deployment from a fixed guide.

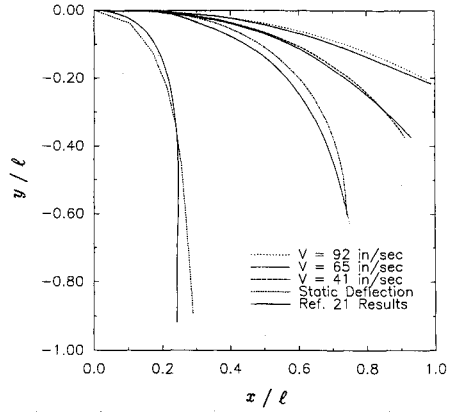

Fig. 5 Beam end orbits for various deployment speeds.

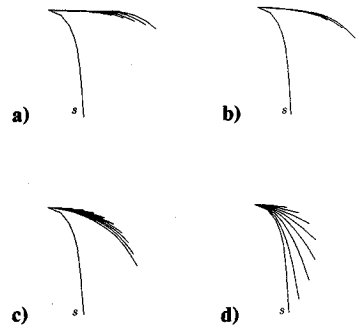

Fig. 6 Beam motion history for various deployment speeds: a) V = 92 in./s; b) V = 65 in./s; c) V = 41 in./s; and d) V = 20 in./s.

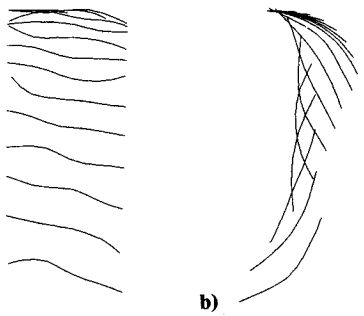

Fig. 7 Free-fall motion history after beam ejection: a) V = 120 in./s; and b) V = 41 in./s.

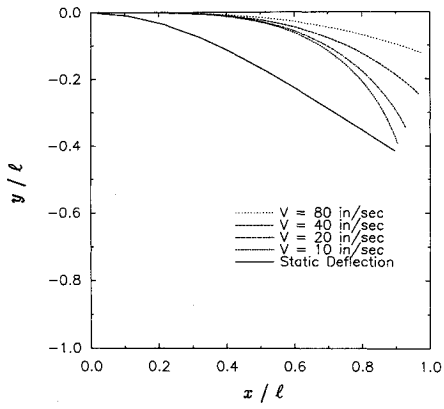

Fig. 8 Beam end orbits for various deployment speeds.

sent formulation are compared with the results of Ref. 21 in Fig. 5 where the end-orbit trajectories normalized by the fully extended beam length (x/ℓ, y/ℓ) have been plotted. The static deformation of a fully extruded cantilevered beam in a uniform gravitational field is also plotted to show the amount of flexibility within the beam and elastica models. In obtaining the present results, six variable length finite elements were used to discretize the beam throughout the deployment, and a cantilever boundary condition was used at the node fixed at the point where the beam ejects from the guide. Nine fixed length constant strain finite elements were used to obtain the static deformation shape. The present nonlinear Timoshenko beam model exhibits deflections that are slightly smaller than the elastica model of Ref. 21; this difference is most pronounced at the slower deployment speeds and the static deflection. For the present formulation, an animated history of the beam deformations throughout various stages of the deployment are shown up to the point when the beam reaches its final length for the various deployment velocities in Fig. 6. In this figure, the deformed beam shapes labeled s correspond

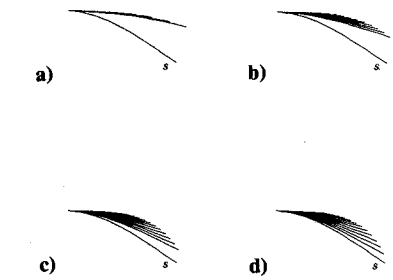

Fig. 9 Beam motion history for various deployment speeds: a) V = 80 in./s; b) V = 40 in./s; c) V = 20 in./s; and d) V = 10 in./s.

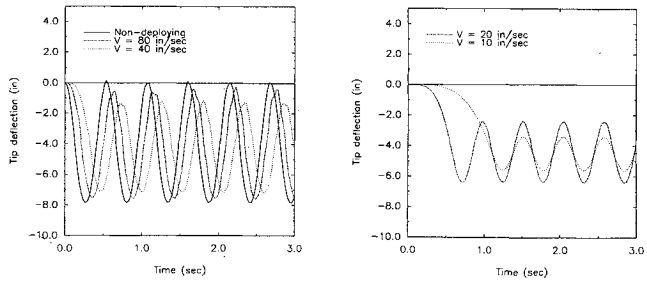

Fig. 10 Beam tip deflections vs time.

to the static shape of a fully extended cantilevered beam, and the increment times between the deformed shapes shown in this figure are 1) 0.012 sec, 2) 0.02 sec, 3) 0.024 sec, and 4) 0.06 sec. The cantilevered boundary condition is removed at the point the beam becomes fully ejected. In Fig. 7, the animated history of the beam motion is extended to show the free-fall motion of the beam after it has left the guide. The increment time between the deformed shapes shown in this figure is 0.03 sec.

A second example is given in which the Young's modulus E has been increased by a factor of 10. In the same manner as in Fig. 5, the normalized beam end orbits throughout the deployment are plotted along with the static deformation shape for this second case in Fig. 8. The animated history of the beam deformations up to the point the beam first reaches its full length is given for various deployment speeds in Fig. 9. In this example, the left beam boundary is kept cantilevered both during and after the deployment stage. To show the beam response both during and after the deployment phase, the beam tip deflection is plotted vs. time for various deployment speeds in Fig. 10.

VI. Concluding Remarks

An effective finite element method has been developed to model the axial deployment of highly flexible beams. The method is based on a geometrically nonlinear beam formulation presented by the authors in Refs. 29-31. A moving finite element reference grid is incorporated within the nonlinear beam formulation to model the deployment motion.The computational methodology is then derived from a space-time finite element discretization of Hamilton's law of varying action. To incorporate the moving node formulation within the internal force computational procedure, the solutions of a past configuration are appropriately extrapolated to the grid representing the current configuration. The present analysis addresses the planar motion of highly flexible beamlike structures being deployed or ejected from a fixed base; a fully three-dimensional analysis of beam ejection from an orbiting base is to be presented in a future work.

Acknowledgments

The work reported herein was supported by the NASA/ Langley Research Center through NASA Grant NAG-1-756

and the NASA Graduate Students Research Program through Grant NGT-50254. The authors wish to thank Jerry Housner for his interest and support during the course of the present work.

References

[1]Carrier, G. F., "The Spaghetti Problem," *American Mathematical Monthly,* Vol. 56, 1949, pp. 669–672.

[2]Sack, R. A., "Transverse Oscillations in Traveling Strings," *British Journal of Applied Physics,* Vol. 5, June 1954, pp. 224–226.

[3]Archibald, F. R., and Emslie, A. G., "The Vibration of a String Having a Uniform Motion Along its Length," *Journal of Applied Mechanics,* Vol. 25, 1958, pp. 347–348.

[4]Swope, R. D., and Ames, W. F., "Vibrations of a Moving Threadline," *Journal of the Franklin Institute,* Vol. 275, No. 1, 1963, pp. 36–55.

[5]Mote, C. D., Jr., "On the Nonlinear Oscillation of an Axially Moving String," *Journal of Applied Mechanics,* Vol. 33, June 1966, pp. 463–464.

[6]Ames, W. F., Lee, S. Y., and Zaiser, J. N., "Non-Linear Vibration of a Traveling Threadline," *International Journal of Non-Linear Mechanics,* Vol. 3, No. 4, 1968, pp. 449–469.

[7]Shi, L. Y., "Three-Dimensional Non-Linear Vibration of a Traveling String," *International Journal of Nonlinear Mechanics,* Vol. 6, No. 4, 1971, pp. 427–434.

[8]Kim, Y. I., and Tabarrok, B., "On the Non-Linear Vibration of Traveling Strings," *Journal of the Franklin Institute,* Vol. 293, No. 6, 1972, pp. 381–399.

[9]Korde, K. R., "On Nonlinear Oscillation of Moving String," *Journal of Applied Mechanics,* Vol. 52, No. 2, 1985, pp. 493, 494.

[10]Barakat, R., "Transverse Vibrations of a Moving Thin Rod," *Journal of the Acoustical Society of America,* Vol. 43, No. 3, 1968, pp. 533–539.

[11]Simpson, A., "Transverse Modes and Frequencies of Beams Translating Between Fixed End Supports," *Journal of Mechanical Engineering Sciences,* Vol. 15, No. 3, 1973, pp. 159–164.

[12]Buffington, K. W., and Kane, T. R., "Dynamics of a Beam Moving Over Supports," *International Journal of Solids and Structures,* Vol. 21, No. 7, 1985, pp. 617–643.

[13]Wickert, J. A., and Mote, C. D., "Classical Vibration Analysis of Axially Moving Continua," *Journal of Applied Mechanics,* Vol. 57, No. 3, 1990, pp. 738–744.

[14]Tabarrok, B., Leech, C. M., and Kim, Y. I., "On the Dynamics of an Axially Moving Beam," *Journal of the Franklin Institute,* Vol. 297, No. 3, 1974, pp. 201–220.

[15]Banerjee, A. K., and Kane, T. R., "Extrusion of a Beam from a Rotating Base," *Journal of Guidance, Control, and Dynamics,* Vol. 12, No. 2, 1989, pp. 140–146.

[16]Cherchas, D. B., "Dynamics of Spin-Stabilized Satellites During Extension of Long Flexible Booms," *Journal of Spacecraft and Rockets,* Vol. 8, No. 7, 1971, pp. 802–804.

[17]Ibrahim, A. M., and Misra, A. K., "Attitude Dynamics of a Satellite During Deployment of Large Plate-Type Structures," *Journal of Guidance, Control, and Dynamics,* Vol. 5, No. 5, 1982, pp. 442–447.

[18]Lips, K. W., and Modi, V. J., "Transient Attitude Dynamics of Satellites with Deploying Flexible Appendages," *Acta Astronautica,* Vol. 5, No. 10, 1978, pp. 797–815.

[19]Lips, K. W., and Modi, V. J., "Three-Dimensional Response Characteristics for Spacecraft with Deploying Flexible Appendages," *Journal of Guidance and Control,* Vol. 4, No. 6, 1981, pp. 650–656.

[20]Modi, V. J., and Ibrahim, A. M., "A General Formulation for Librational Dynamics of Spacecraft with Deploying Appendages," *Journal of Guidance, Control, and Dynamics,* Vol. 7, No. 5, 1984, pp. 563–569.

[21]Mansfield, L., and Simmonds, J. G., "The Reverse Spaghetti Problem: Drooping Motion of an Elastica Issuing from a Horizontal Guide," *Journal of Applied Mechanics,* Vol. 54, No. 1, 1987, pp. 147–150.

[22]Banerjee, A. K., "Order-*n* Formulation of Extrusion of a Beam with Large Bending and Rotation," *Journal of Guidance, Control, and Dynamics,* Vol. 15, No. 1, 1992, pp. 121–127.

[23]Simo, J. C., "A Finite Strain Beam Formulation, The Three-Dimensional Dynamic Problem, Pt. I," *Computer Methods in Applied Mechanics and Engineering,* Vol. 49, No. 1, 1985, pp. 55–70.

[24]Simo, J. C., and Vu Quoc, L., "Three Dimensional Finite Strain Rod Model, Pt. II: Computational Aspects," *Computer Methods in Applied Mechanics and Engineering,* Vol. 58, No. 1, 1986, pp. 79–116.

[25]Simo, J. C., and Vu Quoc, L., "On the Dynamics in Space of Rods Undergoing Large Motions—A Geometrically Exact Approach," *Computer Methods in Applied Mechanics and Engineering,* Vol. 66, No. 2, 1988, pp. 125–161.

[26]Cardona, A., and Geradin, M., "A Beam Finite Element Non-Linear Theory with Finite Rotations," *International Journal of Numerical Methods in Engineering,* Vol. 26, No. 11, 1988, pp. 2403–2438.

[27]Iura, M., and Atluri, S. N., "Dynamic Analysis of Finitely Stretched and Rotated Three-Dimensional Space-Curved Beams," *Computers and Structures,* Vol. 29, No. 5, 1988, pp. 875–889.

[28]Hodges, D. H., "A Mixed Variational Formulation Based on Exact Intrinsic Equations for Dynamics of Moving Beams," *International Journal of Solids and Structures,* Vol. 26, No. 11, 1990, pp. 1253–1273.

[29]Downer, J. D., "A Computational Procedure for the Dynamics of Flexible Beams Within Multibody Systems," Ph.D. Dissertation, Univ. of Colorado, Boulder, CO, Dec. 1990.

[30]Downer, J. D., Park, K. C., and Chiou, J. C., "Dynamics of Flexible Beams for Multibody Systems: A Computational Procedure," *Computer Methods for Applied Mechanics and Engineering,* Vol. 96, No. 3, 1992, pp. 373–408.

[31]Park, K. C., Downer, J. D., Chiou, J. C., and Farhat, C., "A Modular Multibody Analysis Capability for High-Precision, Active Control and Real-Time Applications," *International Journal for Numerical Methods in Engineering,* Vol. 32, No. 8, 1991, pp. 1767–1798.

[32]Avello, A., De Jalon, J. G., and Bayo, E., "Dynamics of Flexible Multibody Systems Using Cartesian Co-ordinates and Large Displacement Theory," *International Journal for Numerical Methods in Engineering,* Vol. 32, No. 8, 1991, pp. 1543–1563.

[33]Sunada, W., and Dubowsky, S., "The Application of Finite Element Methods to the Dynamic Analysis of Spatial and Coplanar Linkage Systems," *Journal of Mechanical Design,* Vol. 103, No. 3, 1981, pp. 643–651.

[34]Yoo, W. S., and Haug, E. J., "Dynamics of Articulated Structures: Pt. I, Theory," *Journal of Structural Mechanics,* Vol. 14, No. 1, 1986, pp. 105–126.

[35]Shabana, A. A., *Dynamics of Multibody Systems,* Wiley, New York, 1989.

[36]Malvern, L. E., *Introduction to the Mechanics of a Continuous Medium,* Prentice-Hall, Englewood Cliffs, NJ, 1969.

[37]Borri, M., Ghiringhelli, G. L., Lanz, M., Mantegazza, P., and Merlini, T., "Dynamic Response of Mechanical Systems by a Weak Hamiltonian Formulation," *Computers and Structures,* Vol. 20, Nos. 1–3, 1985, pp. 495–508.

[38]Peters, D. A., and Izadpanah, A. P., "hp-Version Finite Elements for the Space-Time Domain," *Computational Mechanics,* Vol. 3, 1988, pp. 73–88.

[39]Borri, M., Lanz, M., and Mantegazza, P., "Comment on 'Time Finite Element Discretization of Hamilton's Law of Varying Action'," *AIAA Journal,* Vol. 23, No. 9, 1985, pp. 1457–1458.

[40]Borri, M., Mello, F., and Atluri, S. N., "Variational Approaches for Dynamics and Time-Finite-Elements: Numerical Studies," *Computational Mechanics,* Vol. 7, No. 1, 1990, pp. 49–76.

[41]Borri, M., Mello, F., and Atluri, S. N., "Primal and Mixed Forms of Hamilton's Principle for Constrained Rigid Body Systems: Numerical Studies," *Computational Mechanics,* Vol. 7, No. 3, 1991, pp. 205–220.